

SPATIAL COHERENCE AND FORMATION OF COLLECTIVELY-COUPLED LOCAL NONLINEAR OSCILLATORS IN SQUID GIANT AXONS

GEN MATSUMOTO and HIDEAKI SHIMIZU
*Electrotechnical Laboratory, Optoelectronics Section,
Tsukuba Science City,
Niihari-gun, Ibaraki 305, Japan.*

(Received December 11, 1981; Accepted March 26, 1982)

Abstract

It was experimentally demonstrated that the spontaneous repetitive firing of action potentials occurs in squid giant axons immersed in a 1:4 mixture of natural sea water (NSW) and 550 mM NaCl when the spatial coherence between the voltage noises at any two different locations in the axon becomes complete. Discrete current fluctuations were detected, and both their number and size increased with the increase of the spatial coherence. Voltage noise and spatial coherence were also measured in normal axons to test whether nerve excitation is initiated in normal axons when the spatial coherence exceeds a critical strength.

All these results suggest that (1) the system considered here is constituted of local, non-linear, self-sustained oscillators and the leaky capacitor, (2) the oscillators distributed homogeneously over the axon are interacting in some way, and (3) the interaction becomes stronger as the axon approaches the firing state. The results are consistent with our proposal that action potentials are generated when the interaction exceeds a critical strength, and that the production of action potentials is a spatially local and temporary transition (assisted by outward current) from one dissipative structure with an asymptotically stable equilibrium point to another dissipative structure with a stable limit cycle.

1. Introduction

Nerve membrane is clearly put far from equilibrium. Therefore, nonlinear non-equilibrium thermodynamics [1-4] seems to be one of the most appropriate approaches to understand the electrophysical properties of nerve membrane. Blumenthal, Changeux and Lefever [5] proposed a theoretical model of nerve excitation (the BCL model) on the basis of nonequilibrium thermodynamics. In the BCL model the all-or-none response of nerve excitation can be grasped as a transition from a resting state of a nonequilibrium and stable organization, corresponding to the dissipative structure of Glansdorff and Prigogine [1,2], to an excited state of another stable organization near thermodynamic equilibrium.

Recently, Matsumoto [6] proposed another nonequilibrium model of nerve excitation in which the production of action potentials in axons is a spatially local and temporary transition (assisted by outward local current) from one dissipative structure with an asymptotically stable equilibrium point, to another dissipative structure with a stable limit cycle; the former structure corresponds to the resting state of the axon and the latter one to the state of spontaneous repetitive firing of action potentials (the firing state) [6-14].

Here we report experimental results on spatial properties of nervous activities, with special attention to the membrane current and voltage fluctuations observed at a transition from the resting to the firing state. The transition (the calcium-induced transition: the reason why we call it this will be discussed later in the *discussion*) was evoked by immersing squid giant axons in a proper mixture of natural sea water (NSW) and 550 mM NaCl. Spatial properties of normal axons were also measured in order to examine further whether the usual production of action potentials by applying outward current externally is basically equivalent to the calcium-induced transition. Temporal properties of the transition were reported elsewhere [6, 8, 9, 11–13].

2. Materials and Methods

Materials

Giant axons of squid (*Doryteuthis bleekeri*) were used. The squid were collected in Sagami Bay, transported to our laboratory, and maintained in a small, circular, and closed-system aquarium tank [15, 16]. The squid can survive in the tank for 40–60 days. Axon diameters were between 500 and 750 μm . The majority of the adherent tissues surrounding the axon were removed under a dissecting microscope. The axon was then transferred to a Lucite chamber filled with natural sea water (NSW; pH 8.2). All of the experiments were carried out at room temperature (15–23°C).

Solutions

The external solution was a 1:n mixture by volume of NSW and 550 mM NaCl aqueous solution, where n is a parameter from 0 to 4. Assuming that the concentrations of ionic species in NSW are the same as those given by Hodgkin [17], then in the 1:n mixture the concentrations are:

$$(1) \quad [\text{Na}] = \frac{460 + 550 \times n}{1 + n},$$

$$(2) \quad [\text{K}] = [\text{Ca}] = \frac{550 - [\text{Na}]}{9},$$

$$(3) \quad [\text{Mg}] = 5.3 \times \frac{550 - [\text{Na}]}{9},$$

$$(4) \quad [\text{Cl}] = 550 - \frac{550 - [\text{Na}]}{9},$$

where [j] stands for the millimolar concentration of the ionic species j. Thus, the sodium concentration [Na] can be used to designate the external solution. The Na concentration 530 mM was found to be a critical concentration, above which the axon was in the firing state and below which it was in the resting state [6].

Spatial coherence function for fluctuating membrane voltage measured at two different points along the axon

The spatial coherence function $C_{ab}(f)$ of voltage noise, measured at two different locations, a and b , along the axon, was determined as a function of distance $|a - b|$ in two cases: One is the case (the calcium-stimulating case) when the axon was immersed in a 1:3 or 1:4 mixture of NSW and 550 mM NaCl and the other (the current-stimulating case) when an outward current pulse was applied through an internal electrode with high resistance. In the latter case, the current electrode was prepared by sputtering silica glass on the surface of platinum wire of 50 μm in diameter and 2–3 cm in length. The resistance of the electrode thus prepared was 100–600 $\text{K}\Omega$, which was relatively high compared to the longitudinal resistance of axoplasm along the fiber [18]. The duration of the outward current pulse was 500 msec, and the pulse repetition rate was 0.2 sec^{-1} , to avoid the after-effect of pre-applied current pulse on the axon [19]. The data, 120, 200, 300 and 400 msec, respectively, from the onset of the application of the pulse to the end of pulse, were recorded on a tape recorder (see below).

For both calcium- and current-stimulating cases, two internal platinized-platinum electrodes were inserted longitudinally into the axon from both ends. The tip of each electrode was 0.5 mm; each of the remaining portions was covered with a glass pipette, 70 μm in diameter. The separation distance between the electrodes was a parameter varying from 1 to 40 mm. The length of axon used was 60 mm, which was determined by the length of chamber. The voltage fluctuations picked up at both electrodes were recorded on two channels of an FM tape recorder (Sony Magnescale Inc., type DFR-3415) through a pair of pre-amplifiers (EG & G Princeton Applied Research, model 113). The noise data were processed to get power spectral densities $P_a^v(f)$ and $P_b^v(f)$ of voltage fluctuations at two locations of a and b , cross-power spectral density $P_{ab}^v(f)$, and a spatial coherence function $C_{ab}(f) (= |P_{ab}^v(f)|^2 / P_a^v(f) \cdot P_b^v(f))$, in the following way, using a signal processor Sanei Sokki Co. Ltd., type 7T07A): The data were uniformly sampled at α msec intervals and assembled into data blocks of 1024 points. This implies a $1.024 \times \alpha$ sample per block and a subdivision of the frequency domain in equal intervals, or lobes, of $0.977 \times 1/\alpha \text{ Hz}$ width. The value of α was properly chosen as previously [20–22]. For example, if noise data were analysed in terms of power spectral densities in the frequency range between 2 and 1,000 Hz, we set α to be 0.5 msec. This implies the 0.512 sec sample per block and the subdivision of the frequency domain into equal intervals of 1.95 Hz width. To avoid aliasing and to assure statistical independence of successive data blocks [20–22], the noise records were previously filtered through low-pass and high-pass filters, having through a rate of attenuation of 40 db per decade, set at 1,000 and 2 Hz in this example, respectively. Spectral densities were averaged for 8 to 20 data blocks [20–22].

Membrane current fluctuations and their power spectral densities

Membrane current fluctuations were measured according to Neher and Sakmann [23] in an axon which was covered with a piece of paper moistened with a 1:4

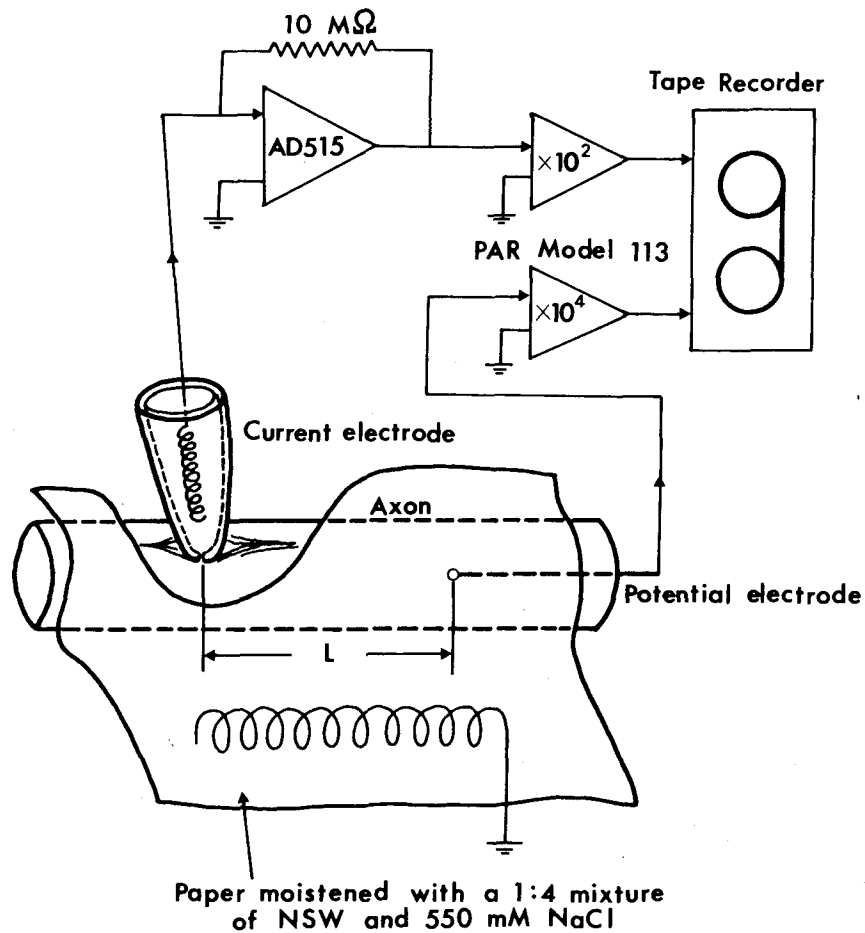


Fig. 1. Schematic diagram for current and potential recordings, from the external surface of squid axon membrane with a fire-polished pipette and from the inside of the axon with a platinized-platinum electrode, respectively.

mixture of NSW and 550 mM NaCl (Fig. 1). The current noise picked up at an area (10^{-4} to 10^{-5} cm 2) of the external surface of the axon was achieved by applying closely the tip of a glass pipette, 50 μ m in diameter, to the axon (Fig. 1). The pipette, which had fire-polished edges, was filled with the 1:4 mixture solution. Its interior was connected to the input of a virtual-ground circuit (Analog Device operational amplifier, AD515), and then to the tape recorder (Sony Magnescale Inc., type DFR-3415) through the pre-amplifier (PAR, model 113).

Spatial coherence between membrane current noise and voltage noise was measured in the same manner as described above by inserting the voltage electrode into the axon longitudinally, where the distance L between the tips of the current and potential electrodes was a parameter.

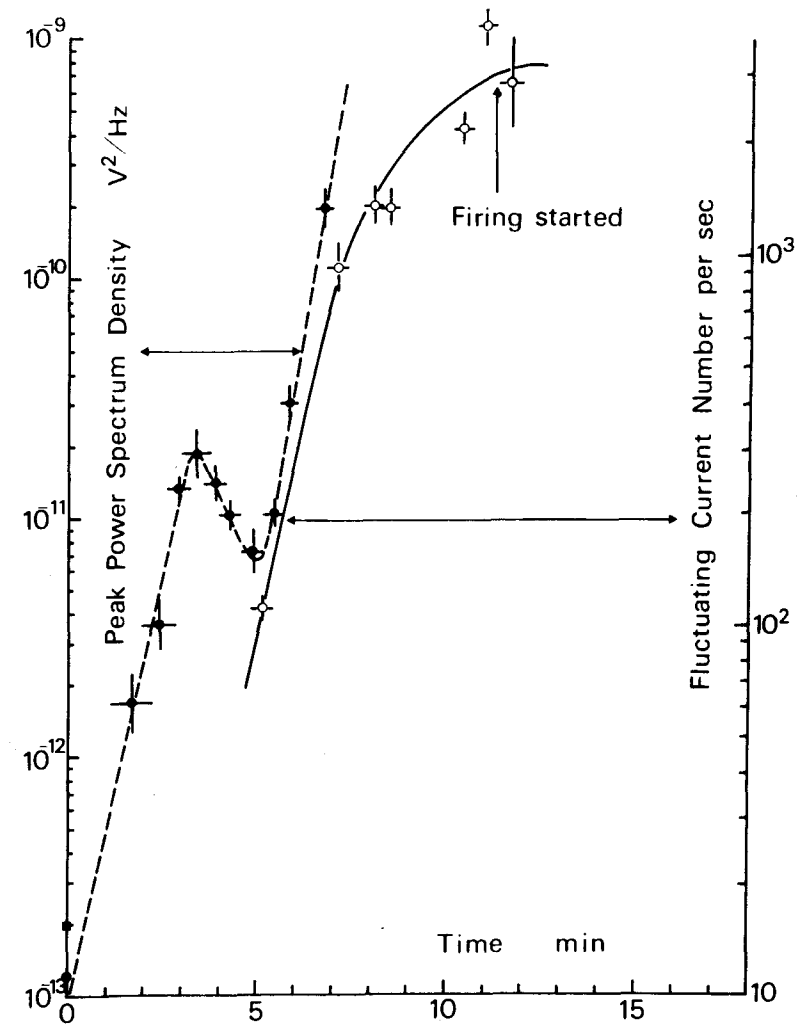


Fig. 2. Peak power spectrum density of the membrane voltage noise (dotted line) and the number of discrete current noise per sec (solid line) as a function of time after the onset of switching the external solution from NSW to a 1:4 mixture of NSW and 550 mM NaCl.

3. Results

Spatial coherence between potential fluctuations detected at two different locations

(A) *The calcium-stimulating case.*—Fluctuating membrane potentials became more oscillatory after the external solution surrounding the axon was switched from NSW to the 1:4 mixture of NSW and 550 mM NaCl, showing a resonance behavior with a center frequency of about 200 Hz at 20°C in the power spectral densities $P^v(f)$ (Fig. 3B), until at last the spontaneous repetitive firing occurred at the repetition frequency of about 200 Hz [6–8, 11, 13, 14]. It should be noticed that it took 10 to 15 minutes until the firing occurred after the external solution was switched from NSW to the 1:4 mixture of NSW and 550 mM NaCl. However, the peak power spectral density around 200 Hz does not increase monotonically as a function of time after the onset of switching the solution from NSW to the 1:4 mixture of NSW and 550 mM NaCl [10]; it initially increased with time, then decreased for a while and finally again continued to increase until the firing took place, as seen in the broken line of Fig. 2.

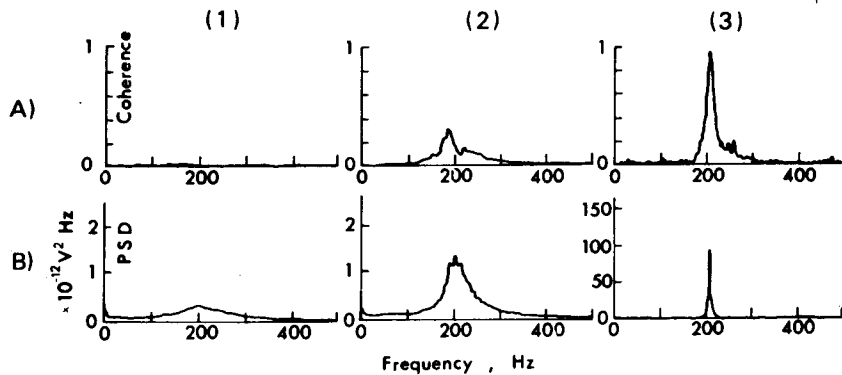


Fig. 3. Spatial coherence between membrane potential noises detected at two locations (separation distance 2.5 cm) (upper column (A)) and power spectral densities of the potential noises detected at one electrode (lower column (B)). The record numbers (1)–(3) shows the spatial coherence and the power spectra, which were processed from the data recorded at 1, 5 and 10 min after the onset of bathing the axon in a 1:4 mixture of NSW and 550 mM NaCl aqueous solution. The firing occurred soon after the data (3) were recorded.

Cross-spectral densities $P_{ab}^v(f)$ between fluctuating potentials detected at two different locations, a and b , in the axon became larger in amplitude at the peak frequency of about 200 Hz and narrower in width as time went on after the onset of switching the solution [6, 8]. These experimental findings were described and discussed in detail in our previous paper [6, 12]. In this report, the spatial coherence function $C_{ab}(f)$ was measured to get more direct information on spatial coherence. Fig. 3A shows the coherence functions thus obtained when $|a-b|=2.5$ cm. The coherence at about 200 Hz (peak coherence) became larger with the increase of the power spectral amplitude at the same frequency (peak power spectral density). The variance of the coherence was usually wider than the spectral width of the power spectral density. The relations between the peak coherence and the peak power

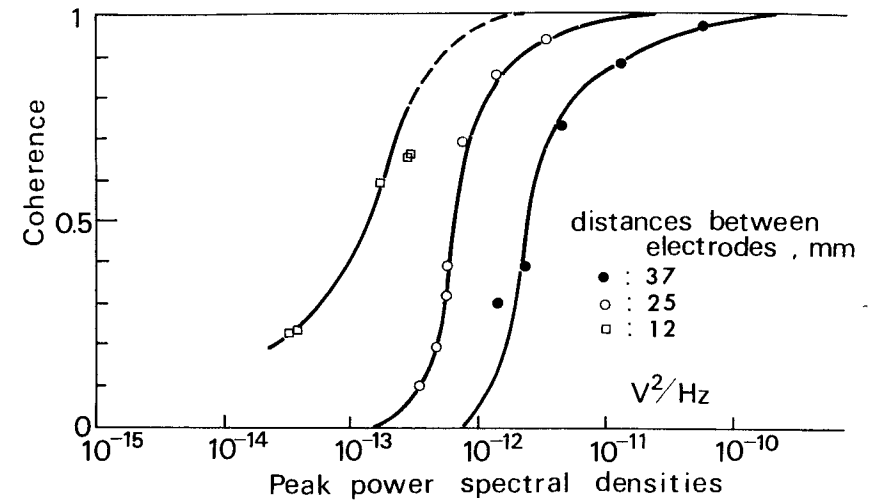


Fig. 4. Relations between the peak spatial coherence and the peak intensities of the power spectral densities of potential noises, as a function of distances between two potential electrodes. The firing did not take place until the peak spatial coherence between potential noises at the distance of 37 mm between two electrodes became close to 1.

spectral density are shown in Fig. 4 for distances $|a-b|$ of 12, 25 and 37 mm, respectively. The data in Fig. 4 were obtained from the same specimen of axon. The spontaneous repetitive firing of action potentials took place after the spatial coherence between two distinct measuring points (e.g., $|a-b|=37$ mm) became very close to 1. This means that firing occurs when the spatial coherence becomes complete all over the entire axon.

(B) *The current-stimulating case.*—Fluctuating potentials became more oscillatory with externally applied outward current, showing a resonance behavior in the power spectral densities (Inset of Fig. 5). In this case, the center frequency in the power spectral densities of voltage fluctuations increased with the current densities (Inset of Fig. 5, Table 1). This should be compared with approximate constancy of the center frequency in the power spectra observed in the calcium-stimulating case [6, 8, 13]. The spatial coherence also increased linearly with the current densities as long as the current density did not exceed $35 \mu\text{A}/\text{cm}^2$ (Fig. 5). It did not depend on the noise data recorded at 120, 200, 300 and 400 msec, respectively, after the onset of application of current pulse of 500 msec in width.

Membrane current noise and spatial coherence between voltage and current noise detected at two different locations

The discrete current noise appeared after a lag phase of time as the external solution surrounding the axon was switched from NSW to the 1:4 mixture of NSW

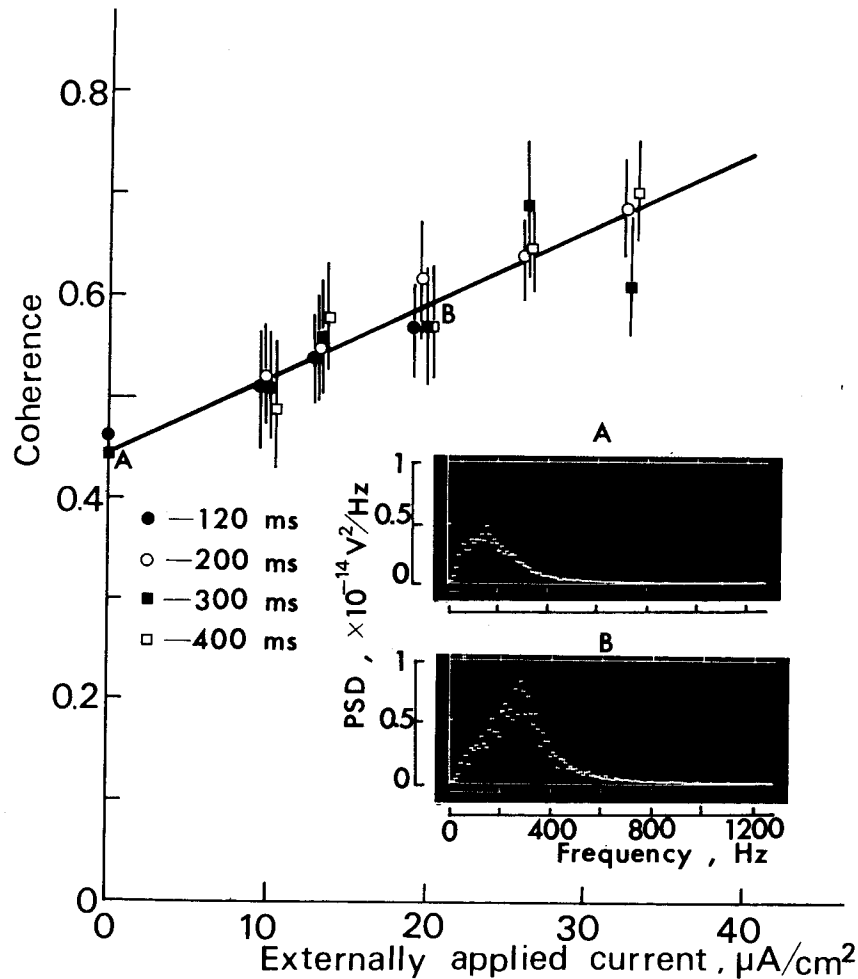


Fig. 5. Dependence of spatial coherence between membrane potential noises detected at two locations (separation distance 1 cm) upon externally applied outward current densities (solid line). The spatial coherences were calculated from the data blocks recorded 120, 200, 300 and 400 msec from the onset and to the end of application of the external current pulse of 500 msec in duration.

Inset: Power spectral densities of potential noises detected at one of a pair of electrodes (upper and lower records) when the external applied outward current densities were 0 (upper picture) and 20 (lower picture) $\mu\text{A}/\text{cm}^2$, respectively.

Current densities ($\mu\text{A}/\text{cm}^2$)	Center frequency in power spectral densities (Hz)	Center frequency in spatial coherence (Hz)
0	219 ± 25	283 ± 25
9.5	225 ± 13	275 ± 13
12.7	238 ± 25	288 ± 38
19.1	269 ± 13	300 ± 13
25.4	263 ± 38	400 ± 38
31.8	281 ± 44	388 ± 40

Table 1. Effect of outwardly flowing current upon center frequencies in power spectral densities of potential fluctuation and in spatial coherence.

and 550 mM NaCl (Fig. 2). The number of the discrete current noise per sec (Fig. 6) increased monotonically with time after the lag phase (usually for 3–6 minutes). The discrete current noise did not disappear even during the firing state and its number per sec seemed to be unchanged or a little less than the one observed just before the firing (see Fig. 2). Amplitude histograms were calculated from the current records to estimate the size of the current pulses, as a function of time after switching the solution (Fig. 6). The amplitudes were measured as the difference

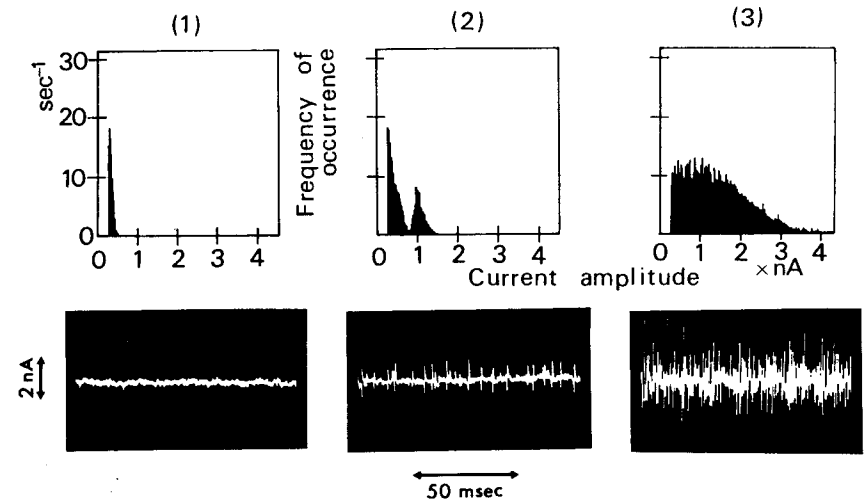


Fig. 6. Fluctuating currents before and after the axon was moistened with a 1:4 mixture of NSW and 550 mM NaCl aqueous solution. Records (1)–(3) were taken for the axon moistened with NSW, 2 and 7 min. after the onset of moistening the axon with the 1:4 mixture, respectively. Upper records stand for amplitude histograms of the current noises, and lower records for oscilloscope traces of the current.

between the outward current peak and the neighbouring inward one, and the frequency of occurrence at a given amplitude was counted when the amplitude exceeded 0.25 nA. Discrete current pulses are those with 0.5 and 1 nA in amplitude. It should be noted that the frequency of occurrence of the discrete pulses of 0.5 nA was almost the same as the 1 nA pulses. The shape of the discrete current pulse was biphasic (Fig. 7); that is, the current first flowed inwardly, and then outwardly. The

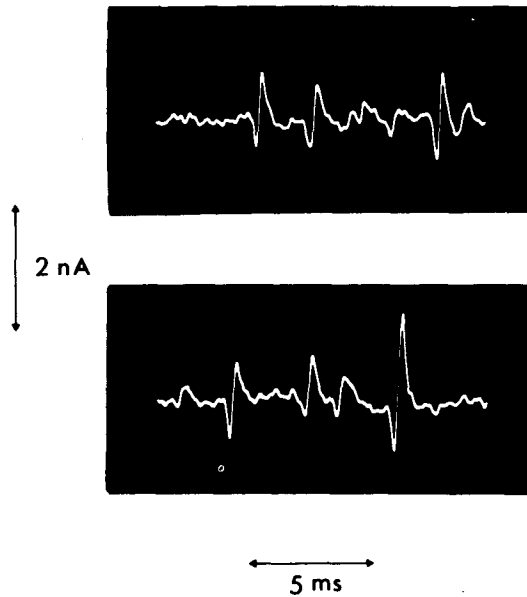


Fig. 7. Discrete current noises corresponding to the record (2) in Fig. 6 as magnified in time-scale.

duration of the pulse was of the order of 0.5 msec. As the axon approached the firing state, the number of discrete current pulses were overwhelming (see Fig. 2), and the amplitude histogram became a continuous spectrum (Record (3) of Fig. 6). Fig. 8 shows power spectral densities of voltage (three upper records) and current (three lower records) noise, and the spatial coherence between the voltage and current noises (three middle records), when the records (1), (2) and (3) were detected 0, 2 and 7 min, respectively, after switching the external solution from to the 1:4 mixture of NSW and 550 mM NaCl. Power spectral densities of current noise showed broad spectra with center frequencies of 500–1,000 Hz. In this figure, the separation distance between the electrodes of voltage and current noise was 1 cm. The spatial coherence between the voltage and current noise did not increase as compared with the one between the voltage and voltage noise (the middle

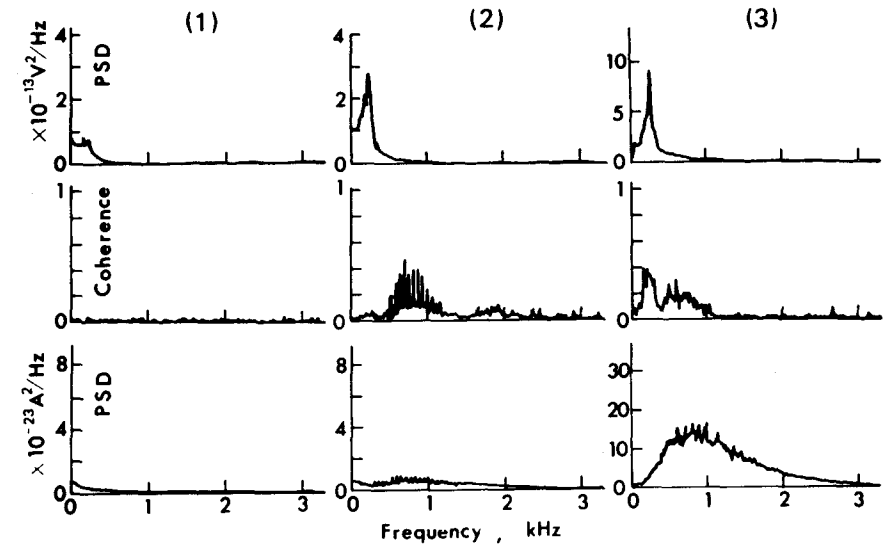


Fig. 8. Power spectral densities of potential (three upper records) and current (three lower records) noises, and the spatial coherences between potential and current noises (separation distance 1 cm: three middle records). The data (1)–(3) for the spectra and the coherences were recorded when the axon was moistened with NSW 2 and 7 min after the onset of moistening the axon with a 1:4 mixture of NSW and 550 mM NaCl aqueous solution.

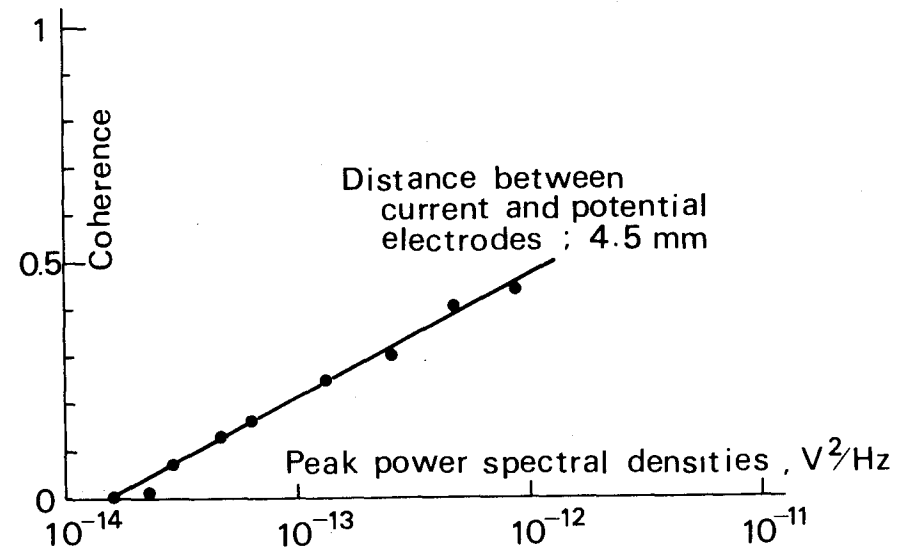


Fig. 9. Dependence of the spatial coherence between the potential and current noises (separation distance 4.5 mm) upon the peak power spectra of potential noise when the axon was moistened with a 1:4 mixture of NSW and 550 mM NaCl aqueous solution.

records of Fig. 8). Fig. 9 shows the relation between the spatial coherence and the peak power spectral densities of voltage noise when the coherence was obtained for the separation distance of 4.5 mm between voltage and current electrodes. The coherence did not increase rapidly with the peak power spectral density as compared with the dependence of the spatial coherence between voltage and voltage noise upon the peak power density (Fig. 4). The spectral densities of current noise are obtained as a convolution of the Fourier transformation of the shape of

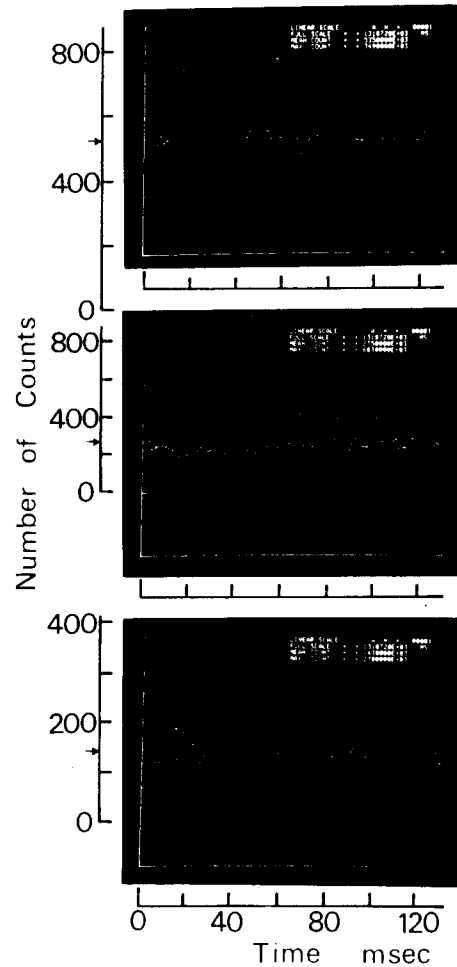


Fig. 10. The auto-correlation of pulse intervals of current noises after the real current noise record was discriminated at different slice levels of 0.25 nA (the upper record), 0.5 nA (the middle record) and 0.7 nA (the lower record), respectively.

discrete current pulses (Fig. 7) and the Fourier transformation of the auto-correlation of the discrete pulse intervals. To eliminate the contribution of the shape of discrete current pulses from the power spectral densities, the current record was processed by our computer-based photoelectron counting system [24] to obtain the auto-correlation function of the pulse intervals after the real record was clipped at different slice or discriminating levels of 0.25, 0.5 and 0.7 nA, respectively (Fig. 10). It should be noted that the spectra are clearly different from the single-exponential decay but discrete. It was found from Fig. 10 and other similar data analyzed with different discriminating current levels that the discrete spectra can be explained by assuming the four basic repetitive current pulses with the repetition frequencies of 25.6, 32.6, 48.9 and 59.7 Hz. This means that the discrete current pulses were spontaneously generated at constant rhythms of the above

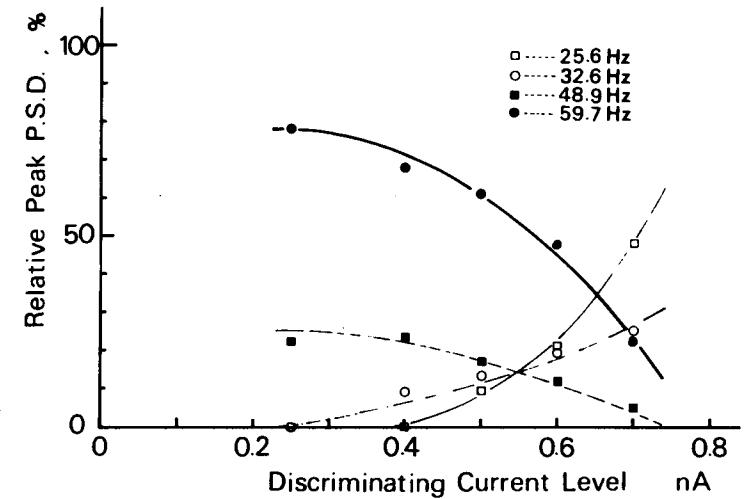


Fig. 11. Relative intensities of the basic frequencies in the repetitive discrete current noises, obtained by the analysis of the auto-correlation data such as those in Fig. 10, as a function of discriminating current levels.

frequencies. The relative intensities of the discrete spectra with 25.6, 32.6, 48.9 and 59.7 Hz were dependent on the discriminating current level (Fig. 11); the lower repetition rate of regenerated current noise becomes overwhelming as the discriminating current level is set at higher levels. This means that the frequency of spontaneous repetitive local currents becomes lower as the current amplitude becomes bigger. The spontaneous repetitive current is not propagated as judged from the shape of current in Fig. 6, since if the local current is of propagated type, first it should flow outwardly, then inwardly as a result of local excitation and finally again outwardly [6].

4. Discussion

The voltage noise with the frequencies around 200 Hz was found to increase with time (the state I) after the onset of switching the external solution from NSW to the 1:4 mixture of NSW and 550 mM NaCl, then to decrease for a while (the state II) and finally to increase again rapidly (the state III) until the firing took place. (Fig. 2). First, we discuss the characteristics of the calcium-induced transition by classifying the transition region into these three states.

The characteristics of the calcium-induced transition

In the state I, the voltage noises increase monotonically with time, but spatial coherence between the voltage noises was close to zero (see the record (1) in Fig. 4) and the discrete current noise could not be observed (Fig. 2). These experimental results show that there are no, or only small if any, collective interactions among local excitatory sites in the state I of axons, as assumed by Hodgkin and Huxley [42] for normal axons. The increase of the power spectrum density of voltage noise with time is explained [12] simply by the phenomenological observation found by Frankenhaeuser and Hodgkin [25] that reducing external calcium concentration by a factor of 5 has the effect of shifting both sodium and potassium conductance-voltage curves about 15 mV toward more negative potentials. In other words, the probabilities that Na and K channels become open increase, even if the resting membrane potential is kept almost constant, independent of the mixing ratio n [6], with the reduction of external calcium concentration from using the mixture solution of NSW and 550 mM NaCl.

In the state II, the power spectrum density of voltage noise decreased with time (Fig. 2) but the spatial coherence began to increase (see the record (2) of Fig. 3). These results show that the voltage noises were suppressed as the local excitatory sites started to interact. It has been established, experimentally and theoretically, that electrical noises in resistively coupled oscillators are suppressed when the coupling becomes stronger [26, 27]. The similar effect of fluctuation suppression has been well known at the phase transition region when the state approaches the critical point as the result of the stronger interactions as compared with thermal agitation [27, 28]. The fact that the noise suppression takes place after a lag phase (see Fig. 2) suggests that the interactions among the local excitatory sites might be governed by some structures inside the axon [29–31]. The interactions may be regulated with the internal calcium ion concentration [29], so that the interaction develops after about 3-min lag since it takes 5–10 min for the internal calcium ion concentration to reach another equilibrium after the external calcium concentration is changed [32].

In the state III, the voltage noise increases until the firing occurs and, at the same time, the discrete current noise begins to be observed (see Fig. 2). The characteristics of this state III are summarized, as follows: (i) the spatial coherence among local excitatory sites rapidly increases and becomes complete all over the isolated axon just before the firing takes place, judged from the voltage noise measurements (see the record (3) in Fig. 3). Here it should be noted that the spatial coherence is

maintained between the voltage and voltage fluctuations (Fig. 3), but not between the voltage and current fluctuations (Figs. 8 and 9). This means that the membrane impedance along the longitudinal axis of axon plays a large role in the spatial coherence. (ii) With increase of the spatial coherence, discrete current noise pulses of 0.5 and 1 nA in amplitude were observed (Fig. 6). The current amplitudes were 100–500 times bigger than those of single-channel currents recorded from membrane of denervated frog muscle fibers [23], from tissue-cultured muscles [33, 34] and from squid giant axon under voltage-clamp [35, 36]. Thus, the observed discrete noise was not due to opening and closing of a single channel, but may be due to simultaneous opening and closing of 100–500 channels coupled collectively. This view is further supported by the following three experimental findings in this report: The first is that, if opening of individual channels is statistically independent, the probabilities of numbers of channels being open simultaneously would follow a Poisson distribution as in the cases of refs. [23], [33] and [34]. But this is not the case (see upper records (2) and (3) in Fig. 6). The second is that, the power spectra should be lorentzian, in other words, the auto-correlation function should be of the single-exponential decay, as expected from the underlying Poisson random process [27]. But this is not the case either. The third is that, the discrete current pulse shapes are biphasic (Fig. 7) and different from those observed in refs. [23] and [25]–[28]. Judging from the shape, the discrete noise current can be considered to be local miniature excitation and is not propagated. As a result the numbers and sizes of collectively-coupled channels increase with increase in the spatial coherence, until and after the spontaneous repetitive firing of action potentials takes place. (iii) The collectively-coupled excitatory sites excite by themselves in repetitive fashions with their respective frequencies (see Fig. 11). As the state approaches the critical point of the calcium-induced transition, both the size and number of the coupled non-linear oscillators increase (Fig. 6). As the size of the coupled non-linear oscillator becomes bigger, its repetition frequencies seem to be lower (Fig. 11).

All these experimental features suggest that: (1) our system considered here is constituted of local, non-linear, self-sustained oscillators and the leaky capacitor of the lipid in the membrane; (2) the oscillators distributed homogeneously over the axon are interacting in some way. Thus, the current I across the membrane could be expressed as

$$(5) \quad I = \left(C \frac{dv}{dt} + \frac{v}{R_L} \right) + \frac{1}{N} \sum_{ij} (\text{coupled non-linear oscillators } i, j)$$

; (3) the Q value of the respective oscillator at the resonance frequency around 200 Hz becomes higher as lower concentration of external calcium ions reduces the membrane resistance at rest [25], and (4) the interaction among the oscillators becomes stronger after a lag phase of time after the axon is bathed in the 1:4 mixture of NSW and 550 mM NaCl. The oscillators could be coupled not only through the pair interaction between limit-cycle oscillators but also through the electrostatic interaction driven by external current to which the leaky capacitor responds [37], or through the diffusion-like interaction caused by the longitudinal

flow of the current along the axon [38]. Our experiments have clarified the importance of the pair interaction to induce megaloscopic limit-cycle in the axon. It can be easily verified that the above equation (5) explains well the power spectrum densities of membrane voltage fluctuations when the axon is immersed in the 1:4 mixture of NSW and 550 mM NaCl [4]. It should be noted here that the general features of coupled non-linear oscillators were studied in detail quite recently [39–41].

In general, long-range spatial cross-correlation was theoretically expected to increase when a far-from-equilibrium system approached its bifurcation point [2]. In our system a critical point of the transition from the resting to the firing state corresponds to the Hopf's subcritical bifurcation point [12]. Therefore, from the standpoint of non-equilibrium thermodynamics, the growth of spatial coherence as the state approaches the critical transition point is a typical spatial feature of the system far from equilibrium. In turn, these facts show that nervous activities are ascribed to typical phenomena as observed in the non-equilibrium system.

In Hodgkin-Huxley terms [42] the characteristics described above make us expect that the slope of the sodium permeability (P_{Na}) curve along the potential axis should increase when the axon is bathed in the 1:4 mixture of NSW and 550 mM NaCl. In this context it is interesting that Brismar [43] found a positive shift of the P_{Na} curve along the potential axis and, at the same time, an increase in the slope of the P_{Na} curve of myelinated nerve fibers of *Xenopus laevis*, by decreasing the divalent cation concentration in the external medium. The positive shift of the P_{Na} curve was first found by Frankenhaeuser and Hodgkin [25] in squid giant axons.

The current-induced transition

Is normal production of action potentials, assisted by outward current, also initiated when the spatial coherence exceeds a critical strength? The spatial coherence increased linearly with externally applied outward current (Fig. 5). The maximum applied current was $35 \mu\text{A}/\text{cm}^2$, which was equal to the rheobase of $35 \mu\text{A}/\text{cm}^2$ [18]. Membrane potentials became more fluctuating with external outward current (the inset of Fig. 5). This had been first discovered by Tasaki [44] who recorded the data blocks 10 sec after the onset of the current with maximum intensity $50 \mu\text{A}/\text{cm}^2$. These experimental findings of the increase of spatial coherence and of voltage fluctuations are consistent with our proposal concerning the onset of normal excitation [6]. A clearer test on the proposal is left for the future study. Most desirable is to record the data blocks immediately after the onset of the external current by avoiding saturation effects upon a pre-amplifier (PAR model 113).

References

- [1]. Glansdorff, P. and Prigogine, I. (1971). *Thermodynamic theory of structure, stability and fluctuations*. Wiley-Interscience, London.
- [2]. Nicolis, G. and Prigogine, I. (1977). *Self-organization in nonequilibrium systems*. Wiley-Interscience, London.
- [3]. Haken, H. (1977). *Synergetics — an introduction. Nonequilibrium phase transitions and self-organization in Physics, Chemistry and Biology*. Springer-Verlag, Berlin.
- [4]. Tomita, K. and Tomita, H. (1974). Irreversible circulation of fluctuation. *Prog. Theor. Physics* **51**, 1731–1749.
- [5]. Blumenthal, R., Changeux, J. P. and Lefever, R. (1970). Membrane excitability and dissipative instabilities. *J. Membrane Biol.* **2**, 351–374.
- [6]. Matsumoto, G. (1981). Long-range spatial interactions and a dissipative structure in squid giant axons and a proposed physical model of nerve excitation. In: *Nerve Membrane, biochemistry and function of channel proteins*. (Ed. by G. Matsumoto and M. Kotani.) The Univ. of Tokyo Press, Tokyo.
- [7]. Matsumoto, G. and Shimizu, H. (1978). A spatially organized structure observed in the time-ordered state of squid giant axons. *J. Phys. Soc. Japan (Letters)* **44**, 1399–1400.
- [8]. Matsumoto, G. and Stühmer, W. (1978). Cross-correlation of fluctuating membrane potentials in squid giant axons. *J. Phys. Soc. Japan (Letters)* **45**, 1069–1070.
- [9]. Matsumoto, G. and Kunisawa, T. (1978). Critical slowing-down near the transition region from the resting to time-ordered states in squid giant axons. *J. Phys. Soc. Japan (Letters)* **44**, 1047–1048.
- [10]. Matsumoto, G. (1978) Current fluctuations observed in squid giant axons. *J. Phys. Soc. Japan (Letters)* **45**, 2047–2048.
- [11]. Matsumoto, G., Kim, K. S., Uehara, T. and Shimada, J. (1980). Electrical and computer simulations upon the nervous activities of squid giant axons at and around the state of spontaneous repetitive firing of action potentials. *J. Phys. Soc. Japan* **49**, 906–914.
- [12]. Aihara, K. and Matsumoto, G. (1982). Temporarily coherent organization and instabilities in squid giant axons. *J. Theor. Biol.* **95**, 697–720.
- [13]. Matsumoto, G., Tasaki, I. and Inoue, I. (1978). Oscillatory subthreshold responses and potential fluctuation observed in squid giant axons.
- [14]. Matsumoto, G. Aihara, K. and Utsunomiya, T. (1982). A spatially-ordered pacemaker observed in squid giant axons. *J. Phys. Soc. Japan* **51**, 942–950.
- [15]. Matsumoto, G. (1976). Transportation and maintenance of adult squid (*Doryteuthis bleekeri*) for physiological studies. *Biol. Bull.* **150**, 279–285.
- [16]. Matsumoto, G. and Shimada, J. (1980). Further improvement upon maintenance of adult squid (*Doryteuthis bleekeri*) in a small circular and closed-system aquarium tank. *Biol. Bull.* **159**, 319–324.
- [17]. Hodgkin, A. L. (1964). *The conduction of the nervous impulse*. Liverpool Univ. Press, Liverpool.
- [18]. Cole, K. S. (1972). *Membranes, Ions and Impulses*. Univ. California Press, Berkeley.
- [19]. Adelman, Jr. W. J., Palti, Y. and Senft, J. P. (1973). Potassium ion accumulation in a periaxonal space and its effect on the measurement of membrane potassium ion conductance. *J. Membrane Biol.* **13**, 387–410.
- [20]. Conti, F., De Felice, L. J. and Wanke, E. (1975). Potassium and sodium ion current noise in the membrane of the squid giant axon. *J. Physiol. (London)* **248**, 45–82.
- [21]. Fishman, H. M., Poussart, D. J. M. and Moore, L. E. (1975). Noise measurements in squid axon membrane. *J. Membrane Biol.* **24**, 281–304.
- [22]. Ohmori, H. (1978). Inactivation kinetics and steady-state current noise in the anomalous rectifier of tunicate egg cell membranes. *J. Physiol. (London)* **281**, 77–99.
- [23]. Neher, E. and Sakmann, B. (1976). Single-channel currents recorded from denervated frog muscle fibres. *Nature* **260**, 799–802.

- [24]. Matsumoto, G., Shimizu, H. and Shimada, J. (1976). Computer-based photoelectron counting system. *Rev. Sci. Instrum.* **47**, 861-865.
- [25]. Frankenhaeuser, B. and Hodgkin, A. L. (1957). The action of calcium on the electrical properties of squid axons. *J. Physiol. (London)* **137**, 218-244.
- [26]. Yoshitoshi, M. and Mori, S. (1972). Noise suppression effect of oscillators by mutual synchronization. *Trans. Inst. Elect. Commun. Eng. Japan* **55A**, 113-120 (in Japanese).
- [27]. Callen, H. B. (1960). *Thermodynamics*. Wiley, New York.
- [28]. Stanley, H. E. (1971). *Introduction to phase transitions and critical phenomena*. Clarendon Press, Oxford.
- [29]. Matsumoto, G. and Sakai, H. (1979). Microtubules inside the plasma membrane of squid giant axons and their possible physiological function. *J. Membrane Biol.* **50**, 1-14.
- [30]. Matsumoto, G. and Sakai, H. (1979). Restoration of membrane excitability of squid giant axons by reagents activating tyrosine-tubulin ligase. *J. Membrane Biol.* **50**, 15-22.
- [31]. Matsumoto, G., Murofushi, H., Endo, S., Kobayashi, T. and Sakai, H. (1983). Tyrosinated tubulin necessary for maintenance of membrane excitability in squid giant axon. In: *Structure and Function of Excitable Cells*. Plenum Press, New York (in press).
- [32]. Blaustein, M. P. (1977). Effects of internal and external cations and of ATP on sodium-calcium and calcium-calcium exchange in squid axons. *Biophys. J.* **20**, 79-111.
- [33]. Nelson, D. J. and Sachs, F. (1979). Single ionic channels observed in tissue-cultured muscle. *Nature* **283**, 861-863.
- [34]. Jackson, M. B. and Lecar, H. (1979). Single postsynaptic channel currents in tissue cultured muscle. *Nature* **283**, 863-864.
- [35]. Conti, F. (1981). Fluctuation analysis of ionic channels in nerve membranes. In: *Nerve Membrane, biochemistry and function of channel proteins*. (Ed. by G. Matsumoto and M. Kotani.) The Univ. of Tokyo Press, Tokyo.
- [36]. Conti, F. and Neher, E. (1980). Single channel recordings of K^+ currents in squid axons. *Nature* **285**, 140-143.
- [37]. Von der Heydt, I., Von der Heydt, N. and Obermair, G. M. (1981). Statistical model of current-coupled ion channels in nerve membranes. *Z. Phys.* **B41**, 153-164.
- [38]. Blumenthal, R. (1975). Instabilities, oscillations and chemical waves in an oligomeric model for membrane transport. *J. Theor. Biol.* **49**, 219-239.
- [39]. Kuramoto, Y. (1981). Rhythms and turbulence in populations of chemical oscillators. *Physica* **106A**, 128-143.
- [40]. Yamaguchi, Y., Kometani, K. and Shimizu, H. (1981). Self synchronization of nonlinear oscillations in the presence of fluctuations, *J. Stat. Phys.* **26**, 719-743.
- [41]. Urahara, K. and Ezaki, S. (1982). Analysis of fluctuation at the critical state of nerve membrane. *Trans. Inst. Elect. Commun. Eng. Japan* (in Japanese) **J65A**, 386-393.
- [42]. Hodgkin, A. L. and Huxley, A. F. (1952). A quantitative description of membrane current and its application to conduction and excitation in nerve. *J. Physiol. London* **117**, 500-544.
- [43]. Brismar, T. (1980). The effect of divalent and trivalent cations on the sodium permeability of myelinated nerve fibres of *Xenopus laevis*. *Acta Physiol. Scand.* **108**, 23-29.
- [44]. Tasaki, I. (1977). Properties of excitable sites in the squid axon membrane as revealed by use of chemical stimulants and a spectrum analyzer. *Japanese J. Physiol.* **27**, 643-655.